Environmental Engineering and Management Journal May 2018, Vol.17, No. 5, 1237-1248
http://www.eemj.icpm.tuiasi.ro/; http://www.eemj.eu

"Gheorghe Asachi" Technical University of Iasi, Romania

ESTIMATION OF VEHICLE EMISSION ON MAINLINE FREEWAY UNDER ISOLATED AND INTEGRATED RAMP METERING STRATEGIES

Jianbang Du*[1], Qing Li[1], Fengxiang Qiao[1], Lei Yu[1,2,3]

[1]*Innovative Transportation Research Institute, Texas Southern University, 100 Cleburne Street, Houston, Texas, 77004, USA*
[2]*Xuchang University, Xueyuan N Rad, Xuchang, Henan, 461000, China*
[3]*Beijing Jiaotong University, 3 Shangyuancun, Haidian District, Beijing, 100044, China*

Abstract

On freeways with multiple on-ramps, it is a common practice to design a ramp metering strategy so as to regulate the entering rates from ramps and minimize the disruptions on the mainline. Most of the existing studies examine the performance of ramp metering on mobility and safety, rather than their impacts on the environment. This paper focuses on the estimates of vehicle emissions along mainline freeways under various ramp metering strategies. Vehicle speed and acceleration rates were measured during a field test along Interstate Freeway I-45 with five on-ramps in Houston, Texas, USA, while the instant vehicle emissions were estimated accordingly. The test was carried out in three scenarios: (1) no ramp metering, (2) isolated ramp metering, and (3) integrated ramp metering. Results show that, the isolated ramp metering strategy yields the highest emissions on freeway mainline among the scenarios . The mobility is significantly improved for the integrated ramp metering strategy, which also significantly contribute to the reduction in total emissions due to the reduced travel time and well-managed queue length on on-ramps. As a conclusion, the integrated ramp metering is with better mobility and environmental effects than the isolated and no metering strategies.

Keywords: air pollution, integrated control, isolated control, ramp metering

Received: October, 2017; Revised final: March, 2018; Accepted: March, 2018; Published in final edited form: May, 2018

1. Introduction

Air pollutants are widely recognized as the substances that adversely affect the global climate, plants and animal species, and public health (Haines et al., 2006). Human activities related air pollutions account for one third to one half of total air pollutions (Vitousek et al., 1997). Based on the NASA's global climate change report, year 2016 ranked as the warmest year on the record, and the sea level has a rise of nearly 200 mm since 1870. Some believe that carbon dioxide (CO_2) plays an important role in such climate changes as a heat trapping gas (Hansen et al., 2010; Onofrei 2017), while since the Industrial Revolution, CO_2 concentration has increased by 30% in the atmosphere (Vitousek et al., 1997). Besides, the ozone molecule (O_3) is one of the ubiquitous air pollutants (DHHS, 1994), while the ground-level ozone is formed by chemical reactions between oxides of nitrogen (NO_x) and volatile organic compounds (VOC) at the presence of sunlight. During year 2015, metropolitan areas such as Washington D.C., Dallas, and Houston met the overdose of ozone molecule (McCarthy and Lattanzio, 2015). Therefore, air pollution is becoming the most challenging issue for environmental sustainability.

In urban areas, about 50% to 90% air pollutions are generated by fuel-combusted vehicles (Shinar, 2017). For instance, Environmental Protection Agency (EPA) reported that on-road vehicle

* Author to whom all correspondence should be addressed: e-mail: dujianbang@gmail.com; Phone: +1 9792291555

emissions are responsible for 41% of the total NO_x emissions in New England area (Weinhold, 2011). The PM2.5 concentrations on the highways with heavier average daily traffic are tremendously higher than with lighter traffic (Li et al., 2018). Brugge et al. (2007) found that, people living close to a freeway (within about 200 m) would be affected by more air pollution than those living at a great distance or close by an urban street. Approximately, 11% of US population is living within 100 m of a 4-lane freeway. The air pollution by the freeway traffic became an critical issue. Traffic activity is one of the factors that influence vehicle's emission rates. Some certain activities like congestion and stop-and-go behaviors could increase the emissions of some pollutants (Franco et al., 2013). For example, Mensik et al. (2000) reported that VOC and NOx emissions from passenger cars during rush hours are 10% and 20% higher than during smooth flow conditions. Frey and Liu (2013) demonstrated that the emissions would increase 50% during congestion.

Certain strategies have been proposed to reduce vehicle emissions, such as the ecology oriented pavement designs, green road operations, road designs, and urban planning (Jaafar 2016; Rosu et al., 2018; Su et al., 2017). For example, emissions could be reduced through careful selection of types and materials. Stiffer pavements like concrete ones could reduce fuel consumption for 3%, which would reduce the total CO_2 emission by 46.5 million tons a year in the United States (Howard and Warren, 2009). The green road operation strategies can smooth the stop-and-go driving behaviors via various countermeasures, such as drivers' smart advisory system (Li et al., 2017a). On the other hand, the driving behaviors are subject to roadway design as well. For instance, weaving areas and merging areas on freeway are the critical segments that may induce the higher frequency of speed changes (Li et al., 2017b). Drivers are more likely to execute frequent small acceleration on the longer route of a roundabout design, while hard acceleration events are often observed on the shortest route (Liu et al., 2017). Besides, vehicle emissions related health effects are considered as one of hidden costs in real estate values and long commutes with fuel combusted vehicles are the major source of air pollution in a metropolitan area (Qiao et al., 2014, 2016).

Ramp meters could reduce the traffic congestion through adjusting the flow of traffic entering freeways to minimize the disruptions on mainline traffic flows from ramps (Arnold Jr, 1998). As a result, non-recurrent congestions caused by crashes could be relieved, leading to emission reductions (Hall and de Hurtado, 1992; Wu et al., 2017). However, there are fewer studies on the specific impacts of ramp metering on freeway emissions.

The objective of this research is to explore the impacts of isolated and integrated ramp metering strategies on the emissions in mainline freeways. The emissions were estimated by MOVES based on the instant vehicle speed and acceleration rate, that were measured from a test vehicle driving along the freeway I-45 in Houston, Texas, where five on-ramps were placed with three control scenarios: (1) no metering, (2) isolated metering, and (3) integrated metering.

2. Ramp metering strategies

A ramp meter is typically installed on a freeway entrance ramp to regulate the traffic flow entering a freeway according to actual traffic conditions, in terms of the queue length on the ramps at the upstream and the demands on the freeway mainline and merge points. The ramp meter is consisted of a signal head, detectors and a signage.

There are either two (red and green), or three (red, yellow, and green) phase indications in the signal head (Papageorgiou and Kotsialos, 2000), while the detectors monitor the traffic conditions on the ramp and the freeway mainline to determine the metering rate. The detectors on the freeway mainline and on the ramps are connected to the ramp controller cabinet. The signage is the signal light placed at the stop line of the ramp as a sign on whether the ramp is being metered at the time (Arnold Jr, 1998). When the ramp meter was working, vehicles travel from an adjacent service road line up a queue behind the stop bar on the ramp and wait for the right of way to enter the freeway. There are generally two different strategies for ramp metering, namely isolated control strategy and integrated control strategy (Bhouri et al., 2013).

2.1. Isolated ramp metering

An isolated ramp metering control strategy monitors the traffic conditions of the ramp and the nearby freeway mainline segments. This strategy is intended to maintain the traffic flow in the mainline at a constant level (Cassidy and Rudjanakanoknad, 2005), which was mostly designed for localized problems to react to traffic conditions. However, an isolated ramp meter does not communicate and share information with each other in a traffic network, which thus can only be controlled and operated individually (Guang and Lei, 2006). Fig. 1 shows an isolated traffic responsive ramp meter.

The metering rate of an isolated control ramp meter responds to the local detectors on ramp and adjacent freeway segments (Kachroo and Ozbay, 2011). As Fig. 1 shows, the demand on mainline freeway is detected by a control variable detector, while the om-ramp queue size is triggered by the queue, check-in and check-out detectors (Qiao, 1991). The algorithm of the isolated control ramp metering rate is shown as Eq. (1):

$$x < C - D \quad (1)$$

where: x is the metering rate of an isolated ramp meter in vehicle per hour, C is the capacity of a freeway segment, D is the demand of the upstream traffic of a freeway.

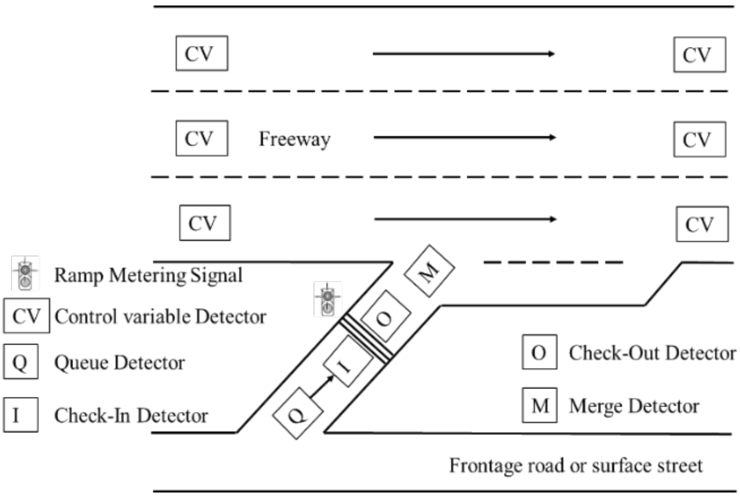

Fig. 1. Isolated traffic response ramp meter

2.2. Integrated ramp metering

An integrated control strategy determines the metering rates based on the mainline vehicle density, mainline required density, and the number of vehicles that needs to be removed or added to the mainline along all ramps (Mahajan et al., 2015). This strategy was designed for system-wide problem solving and could respond to dynamic traffic conditions. The advantage of the integrated control strategy is that the information collected from different ramp metering detectors gathered in a system and processed systemically (Papamichail et al., 2008). This feature could ensure the integrated control strategy to respond to non-static conditions more effectively and systematically (Papamichail et al., 2008).

As Fig. 2 shows, there are n metered ramps along the freeway segment and they separate the freeway into n sections, each section has a capacity. The approach of an integrated control ramp metering rate can be written in a linear programming problem as Eqs. (2-4):

Objective:

$$Maxiumum\left(D_0 + \sum_{i=1}^{n} x_i\right) \tag{2}$$

Subject to:

$$D_0 \times p_{1,j} + \sum_{i=1}^{n}\left(x_i \times p_{i,j}\right) \le C_n, \forall\ j = 1,2,...,n, \tag{3}$$

$$0 \le x_i \le D_i, \forall\ i = 1,2,...,n. \tag{4}$$

where: x_i - the ramp metering rate of ramp number I, vehicle per hour, D_0 - the initial traffic demand approaching the first ramp, D_i - the demand of ramp number i, C_j - capacity of section boundary j, $p_{i,j}$ is the proportion of demand i passing section boundary j.

The algorithms to solve a linear programing problem as illustrated in Eqs. (2-4) have already been well documented in many previous studies, such as Simplex algorithm, Branch and Bound Algorithm and Cutting-plane Algorithm, etc. The readers may refer to (Nash and Sofer, 1996; Luenberger, 1973) for details.

Existing research show that ramp metering strategies could improve the freeway safety and decrease the traffic accident rate significantly. For example, collisions reduced by 35% in Portland and 50% in Denver for the application of ramp metering strategies. Furthermore, ramp meters could influence vehicles' emissions (Pasquale et al., 2014). For example, Minneapolis identified a net annual saving of 1,160 tons of emissions and Denver reduced 20% emissions by the installation of ramp meters. On the other hand, ramp meters require a fully stop at the stop bar, and based on the rates of the ramp meters, vehicles need to stay in a queue on the ramp to wait for entering the freeway mainline (Papageorgiou and Kotsialos, 2000). These driving behaviors would result in increasing vehicles' emissions. On the other hand, ramp meters could reduce the traffic congestion on the mainline, thereby shortening the travel time and eliminate stop-and-go events (Carlson et al., 2010).

3. Vehicle emission estimation

Vehicle emissions could be measured while driving on-road or in a laboratory environment. For the on-road emission tests, a Portable Emission Measurement System (PEMS) and remote sensors are often used to detect the emission rates directly from the tailpipe of a vehicle, and the total emissions from massive vehicles in an area, respectively. However, these measurement approaches are costly and time consuming. In the laboratory environment, chassis and engine dynamometer are usually used to monitor speed profile and gear change, and collect the emissions from a test vehicle to a bag. Nevertheless, the laboratory test does not take into account actual traffic situations (Pierson et al., 1990). A number of emission models and emission factors have been developed to simplify the emission estimation process (Outapa, 2017).

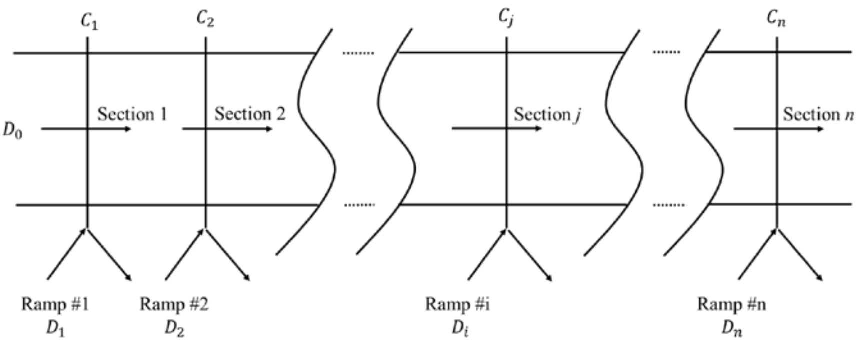

Fig. 2. Freeway segment with integrated control ramp meters

The most predominant model is the Motor Vehicle Emission Simulator (MOVES), which has been approved by the United States Environmental Protection Agency (EPA, 2011). By MOVES, the main traffic related independent variables include driving speed, acceleration rates, and vehicle specific power (VSP), which are easily obtainable in an on-road driving test. More specifically, vehicle emissions are subject to dynamic vehicle operating modes, which were defined by MOVES into 23 bins according to real-time driving speed and VSP. Table 1 shows the specification of the 23 bins, in response to four major emission components from a five-year-old gasoline light duty vehicle, including CO_2, NO_x, carbon monoxide (CO), and hydrocarbon (HC) (Frey and Liu, 2013).

In Table 1, vehicles' operating modes were classified by real-time driving speeds, acceleration rates, and VSP. The VSP is an instantaneous tractive power per unit vehicle mass, which is the sum of power consumption, including aerodynamic drag, acceleration, rolling resistance, and grade, divided by the mass of the vehicle (Pease, 2010). The VSP mathematical formula can be represented by Eq. (5).

$$VSP = v * [1.1 * a + 9.81 * grade(\%) + 0.132] + 0.000302 * v^3 \quad (5)$$

where: v is vehicle speed in m/s, a is acceleration in m/s^2, *grade* (%) is the vehicle vertical rise divided by slope length.

Table 1 has been widely used in gasoline light-duty vehicle emission studies. For example, Li et al. (2016) conducted multiple driving simulator tests to investigate the impacts of a Drivers Smart Advisory System on vehicle emissions in a work zone area.

Subjects' real-time driving speeds were used to classify into operating mode bins for emission estimations. Another example is the floating car test conducted on passenger-picking-up vehicles at airport terminals (Qiao et al., 2015). The vehicles' driving speeds were recorded by a Global Positioning System (GPS), based on which the number of corresponding operating bins were calculated for emission estimation.

Table 1. Operating mode bin on average emission rates for 5-year-old gasoline passenger cars (Frey and Liu, 2013)

Operational Mode ID	***Operation Mode Description (a_t in mi/h/s and v_t in mph)***		***Average Emission Rate (g/h)***			
			CO_2	***NO_x***	***CO***	***HC***
0	Braking/ Deceleration	$a_t \leq$-2.0 OR (a_t < -1.0 AND a_{t-1}<-1.0 AND a_{t-2}<-1.0)	3,529	0.23	5.14	0.19
1	Idling	-1.0 ≤ v_t<1.0	3,265	0.1	0.89	0.05
11	VSP < 0	1≤v_t<25	5,134	0.34	17.69	0.13
12	0≤VSP < 3		7,089	0.52	28.88	0.1
13	3≤VSP < 6		9,852	1.22	26.62	0.19
14	6≤VSP < 9		12,449	2.15	38.2	0.26
15	9≤VSP < 12		14,845	3.81	55.39	0.36
16	12≤VSP		17,930	7.94	93.47	0.58
21	VSP < 0	25≤v_t<50	6,985	0.67	23.05	0.2
22	0≤VSP < 3		7,950	1.09	30.55	0.18
23	3≤VSP < 6		9,683	1.65	39.28	0.2
24	6≤VSP < 9		12,423	2.79	57.42	0.38

25	9≤VSP < 12		16,578	3.91	65.17	0.37
27	12≤VSP < 18		21,855	6.16	97.87	0.59
28	18≤VSP < 24		29,459	13.54	239.24	3.84
29	24≤VSP < 30		40,359	23.78	506.67	6.81
30	30≤VSP		50,682	31.29	1,779.51	11.25
33	VSP < 6		9,951	1.44	17,031	0.19
35	6≤VSP < 12		15,956	3.96	29.56	0.27
37	12≤VSP < 18	$50 \leq v_t$	20,786	5.54	43.51	0.34
38	18≤VSP < 24		27,104	11.5	219.28	2.59
39	24≤VSP < 30		36,102	17.12	231.37	3.76
40	30≤VSP		46,021	21.56	679.99	4.92

4. Methods

On-road driving tests were conducted on a highway, which undergoes three ramp metering conditions: from absent ramp metering, to isolated ramp metering, and then integrated ramp metering strategies. Vehicle emissions were estimated based on the vehicle activity information and the emission rate in Table 1. The vehicle emission patterns and total emissions from a test vehicle under the three scenarios were compared, while the significant differences among the scenarios were examined by statistic tests (Tang et al., 2017).

4.1. Test plan and data collection

Two segments on Interstate Freeway I-45 with the posted speed limit 120 km/h (75 mph) in Houston, Texas, were chosen for on-road driving tests, including the Northbound and Southbound segments between Crosstimber Street and West Road (Fig. 3a). Each segment is about 13.50 km (8.38 miles) long and has been controlled by 5 isolated ramp meters for years. The meters were uninstalled in May, 2017, for system upgrading, including new controllers and integrated metering strategy. Since June 2017, the upgraded integrated ramp metering serves at the two segments. Therefore, the on-road driving tests were carried out on the two segments in March, May, and June, 2017, for three scenarios including absent ramp meters, isolated ramp metering control, and integrated ramp metering control. The absent ramp meter or no control scenario serves as a baseline.

An experienced young driver was recruited to drive a light-duty vehicle, 2014 TOYOTA 4 Runner with 4,000cc displacement and 6,300lbs in weights, along the test routes shown in Fig. 3a during morning (7:30 to 9:00 am) and afternoon peak hours (4:30 to 7:00 pm) of sunny weekdays. The Level of Service (LOS) of the test periods could range from D (with the density close to 22.5 vehicles per km per lane) to F (with the density greater than 22.5 vehicles per km per lane). During driving tests, dynamic traffic conditions were recorded by a dash camera mounted on the windshield, and the geolocations for each 1/10 second were collected by a GPS device , and driving speeds for each second were collected by a computer connected to the On-board Diagnostics (OBD) II port of the test vehicle. Fig. 3b shows the placement of these devices within the test vehicle.

As Fig. 3a shows, the test driver started from the ramp on Crosstimber Street to I-45 towards The Woodlands, Texas, got off at the exit for West road, then made a U-turn and get on to the Southbound of I-45 heading to the exit for Crosstimber Street. A total of 300 km driving distance was covered along the test route under three ramp metering scenarios.

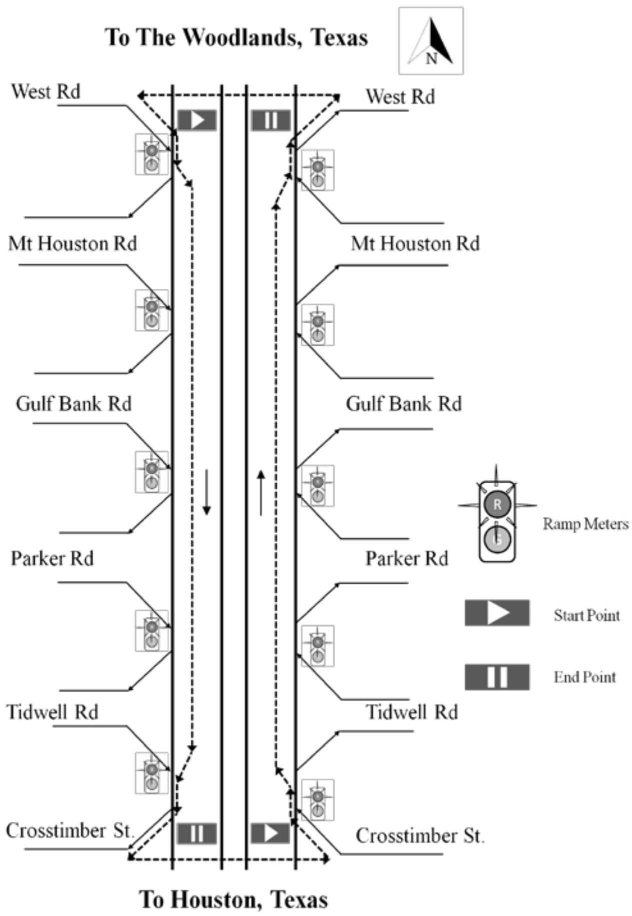

(a)

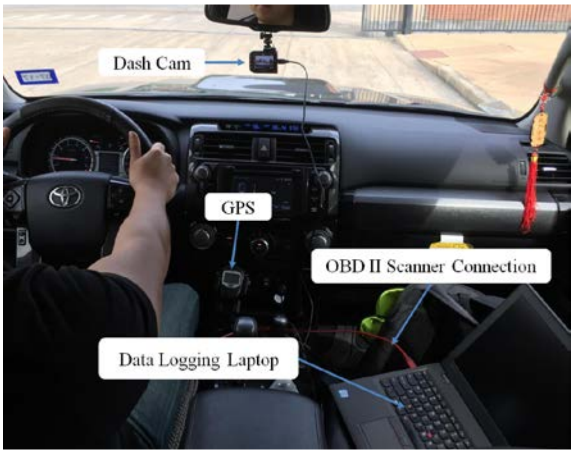

(b)

Fig. 3. Test route and device displacement: (a) Test Route on I-45 South and North Bounds; (b) Device placement within the test vehicle

4.2. Data processing

The collected geolocation information from a GPS was synchronized with the driving speeds from the OBD II. Only the data collected on the mainline of I-45 were retrieved and further divided into three groups based on their onsite ramp metering status related to relevant scenarios.

During data processing, it was found that, the collected traffic conditions and ramp meter allocations on the two segments, Northbound and Southbound, are similar to each other. Two null hypotheses were assumed that, the driving speeds and vehicle emission rates on the two segments under the same scenario come from normal distributions with equal means, and derive from normal distributions with the same variance. The two null hypotheses were tested by one-way ANOVA test and *F*-test with the confidence interval 97%, respectively. Insignificant difference between the two segments implies that the two segments could be deemed as one test site and each complete driving test generates two datasets for the same scenario. Otherwise, each segment is considered as a test site. Meanwhile, the significant different tests among the three scenarios were conducted by one-way ANOVA as well.

The test vehicle's trajectory on the two segments was retrieved by interpolating second-by-second driving speed into spatial domain speed with a 100-m interval. Meanwhile, the time series driving speed in each dataset was used to calculate corresponding acceleration rate and then VSP. As the test site is located in the plain freeway, the grade in Eq. (5) was determined as zero in VSP calculation.

The calculated acceleration rates and VSP, together with driving speed, were adopted to classify the test vehicle's operating mode IDs and estimate four real-time emissions using Table 1. The total vehicle emissions for each emission component are the sum of the products of emission rates and their corresponding time intervals.

5. Results and discussion

Table 2 shows the significant different test results of driving speeds and emission rates on the Southbound and Northbound, under three scenarios. In Table 2, no *p*-value smaller than the significant interval 3% was observed in the ANOVA test as well as F-test, crossing all three scenarios. Thus the null hypotheses of equal means and variances are accepted. This means, the Northbound and Southbound could be considered as one test site in this emission study. Information from both directions are then combined together for the analyses and discussion regarding the impacts of isolated and integrated ramp metering strategies on vehicle emissions and mobility in the entire test site.

5.1. Speed profile analysis

Fig. 4a demonstrates the speed profiles of the three scenarios, namely no ramp metering in green, isolated metering in red, and integrated metering in blue. While the solid lines represent the mean driving speeds, the shades in the corresponding colors indicate relevant standard deviations.

Commonly, there is a slight decline in driving speeds around 35 m, and then a steady increase in the three scenarios, in which drivers just completed merging to the mainline traffic flow. At about 14,500 m away from the start point, a significant drop is observed, where a HOV entrance is allocated and drivers confronted with traffic flow weaving to the HOV lane. Differently, the speed profiles for the ramp metering controls in blue and red, are visibly smoother than the one for the no-control scenario. It seems that drivers frequently conduct a stop-and-go activity when a ramp meter is absent.

Generally speaking, the blue line for the integrated control scenario (79.44 $\pm$ 11.62 km/h) lies above other two lines at the first three quartiles of travel distance, and the driving speeds in the no metering (66.69 $\pm$ 10.28 km/h) and isolated metering scenarios (70.26 $\pm$ 9.19 km/h) are relatively close to each other along the test route. Likewise, the blue shade for the standard deviation (SD) for the integrated metering scenario is obviously larger than the green and red shades for the other two scenarios. The speed variance for the no metering scenario is relatively close to the isolated one. The variances could vary with the actual level of travel demand. The larger variance by the integrated metering indicates its more sensitivity to the traffic flow, in terms of mobility improvement. Further, one-way ANOVA tests show that the three speed profiles are statistically different from each other (No Metering vs. Isolated: p = 9.05E-09; No Metering vs. Integrated: p = 4.52E-65; Integrated vs. Isolated: p = 5.97E-40). This implies that the ramp metering strategy could significantly improve the mobility on average, and the improvement from the integrated ramp metering is more significant than from the isolated ramp metering.

Table 2. Statistically significant test results between northbound/southbound emissions and speed

Scenario	***Test***	***CO_2***	***NO_x***	***CO***	***HC***	***Speed***
		p-value	***p-value***	***p-value***	***p-value***	***p-value***
No Control	ANOVA	0.468	0.930	0.553	0.654	0.673
	F Test	0.036	0.518	0.118	0.272	0.653
Isolated	ANOVA	0.429	0.286	0.528	0.371	0.074
	F Test	0.848	0.803	0.041	0.420	0.149
Integrated	ANOVA	0.363	0.099	0.445	0.298	0.265
	F Test	0.301	0.050	0.187	0.046	0.205

Note: the confidence level is 97%

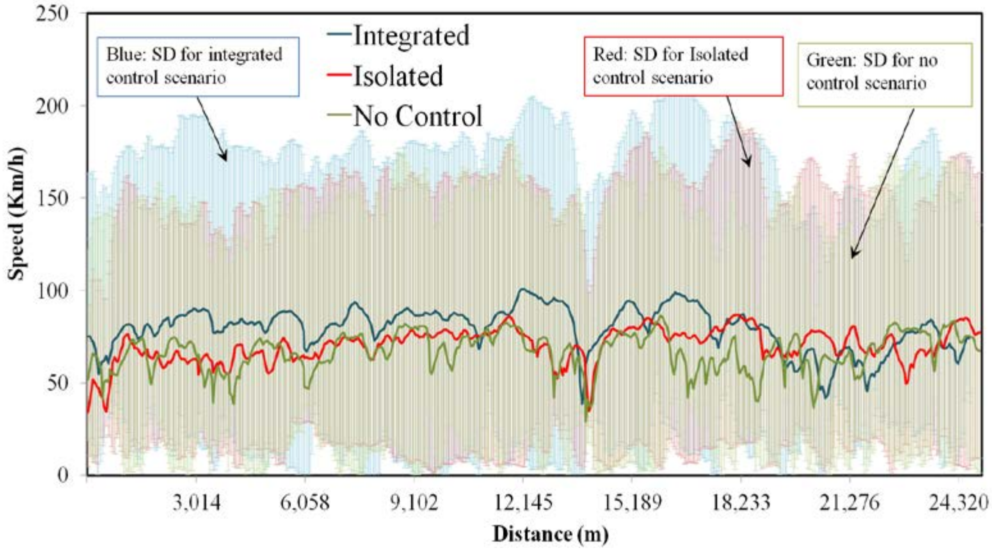

(a)

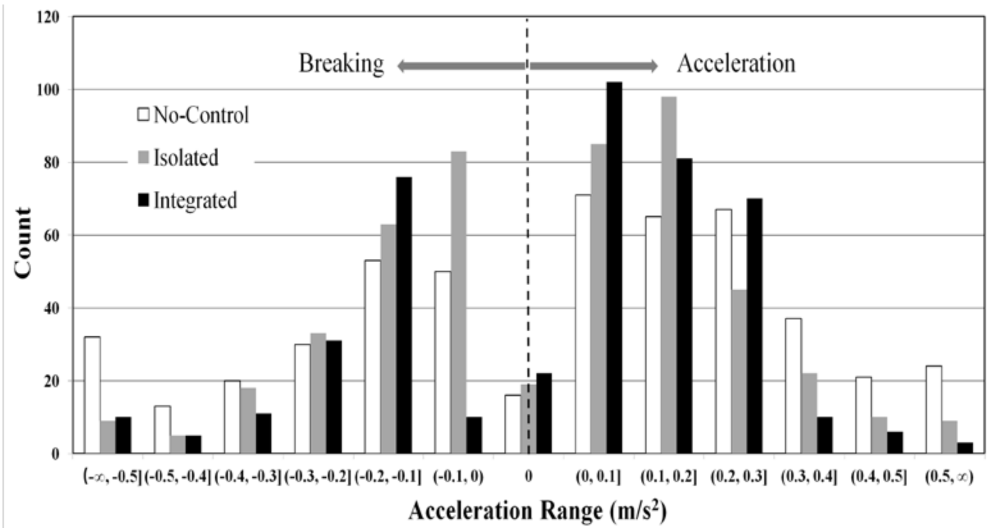

(b)

Fig. 4. Speed profiles and acceleration distributions of different scenarios: (a) Speed profiles of different scenarios; (b) Acceleration distributions (Note: SD is the standard deviation)

5.2. Travel delay analysis

By calculation, when a ramp meter is absent, there is an average of 10.56 min delay with 78.65% longer travel time compared with the free flow status. The installation of the isolated ramp metering control shortens the delay to 8.4 min.

The delay is further shortened by the integrated ramp metering control to only 1.9 min with 14% longer travel time, still compared with the free flow status.

5.3. Acceleration profile analysis

Emission rates are highly sensitive to vehicles' instant acceleration. The harder acceleration could instantly yield higher CO_2 emission rates, while the higher NO_x and HC emission rates are the signs of harder decelerations (Li et al., 2017b). Fig. 4b shows the acceleration/deceleration rate distributions of the three scenarios.

Apparently, the acceleration rates mostly concentrate on the range between -0.3 and 0.3 m/s^2. Comparatively, the acceleration distribution in the no metering scenario is flatter, closed by the ones in the isolated one, and then the integrated one. Regarding the relatively harder acceleration (greater than 0.3 m/s^2), the distribution in the no metering scenario is obviously higher than the ones in the other scenarios, and the distribution in the integrated ramp metering is relatively smaller than the one in the isolated scenario. With respect to the relatively harder deceleration (smaller than -0.3 m/s^2), the distribution in the no metering scenario is similarly higher than the ones in other two scenarios; and the distribution in the integrated scenario is lower than in the isolated scenario.

Thus, the acceleration distributions suggest that, without a ramp meter, drivers would more frequently exert harder acceleration and deceleration, which is consistent with the stop-and-go activity presented in its speed profile in Fig. 4(a). Under an integrated ramp metering strategy, vehicles' acceleration pattern is smoother than under an isolated control. The smoother acceleration patterns may make a great contribution to emission reduction.

5.4. Operational mode analysis

As Table 1 shown, vehicle emission rates are highly associated with its real-time operational modes. Fig. 5 illustrates the operational mode ID distributions performed by the test vehicle under three scenarios.

In Fig. 3, bins zero and one are the braking/deceleration and idling mode, respectively, and other operational modes could be divided into three speed zones; (1) lower speed zone between 1.6 km/h and 40.2 km/h (1-25 m/h), (2) medium speed zone between 40.2 km/h and 80.4 km/h (25-50 mph), and (3) higher speed zone 80.4 km/h above (equal to and greater than 50 m/h). The bin zero bars show that the test driver is more likely to operate braking or deceleration in the no metering scenario, and the least in the integrated ramp metering scenario, which is consistent with the speed profile and acceleration distribution analyses results mentioned earlier. Besides, less than 2% of travel time was spent on bin one (the idling mode) of the integrated scenario, whereas the durations of the idling mode are obviously higher in the scenarios of isolated and no metering strategies with 7% and 9.5%, respectively. The longer idling duration is in accordance with the less mobility presented in speed profiles as well.

In each speed zone, vehicles' VSP increases within a specific speed range as shown in Table 1. In Fig. 5, there is a common trend within each speed zone that the ID distribution declines with the increase of VSP. Moreover, most operational mode IDs under the ramp meter controls tend to distribute to the lower VSP bins within each speed zone, indicating the less power demand for the same driving speed range. To some extent, the ramp metering strategy could improve fuel efficiency. Strikingly, the test drivers spent 43.8% of travel time on the high speed in the integrated scenario, especially with the lower VSP bins (between bins 33 and 37), which is noticeably higher than the ones in the isolated and no metering scenarios with about 17.5% and 7.5%, respectively. The most operational mode IDs distribute to the medium speed zone under the scenarios isolated and no metering, with 62.23% and 61.73%, respectively. Only 39.36% of the operational mode IDs distribute to the medium speed zone under the integrated scenario.

5.5. Emission rate analysis

The distribution of the test vehicle's real-time emission rates under the three scenarios is illustrated in Fig. 6. In Fig. 6, the Interquartile Ranges (IQRs) for the CO_2 emission rates are tremendously greater than the ones for other emissions, indicating higher variability, which is followed by NO_x emissions. Comparatively, the IQR as well as the median level of CO_2 emission rates for the integrated scenario are slightly higher than the ones in the isolated and no metering scenarios, which could be explained by the higher distributions to the lower VSP bins in high speed zone, shown in Fig. 6.

The HC and NO_x emission rates evidently distribute denser at a median level of 0.5 g/h and 2.5 g/h, respectively. Furthermore, the significant difference in the emission rates were tested among the three scenarios and shown in Table 3. Table 3 shows that the four emission components are statistically significant between the no metering and isolated/integrated ramp metering scenarios with the conference interval 97%. Between the two ramp metering strategies, the CO_2 and NO_x emission rates are significantly different from each other, whereas the CO and HC emission rates are statistically insignificant. Therefore, the ramp metering strategy could significantly alter emission rate distributions. Between the isolated and integrated scenarios, the changes in CO_2 and NO_x emissions are significant as well, but rarely presented in CO and HC emissions.

5.6. Total emission analysis

Seemingly, the ramp metering controls could raise high emission rates. Nevertheless, the mobility is significantly improved under the ramp metering controls, which means the emission duration reduce dramatically. As a result, lower total emissions under the isolated and integrated ramp metering controls are expected. Table 3 shows the total emissions in the three scenarios.

As a whole, the total emissions in the integrated scenario are the lowest in the four emission components, which are 15.86%, - 0.37%, 23.35%, and 14.29% lower than the ones in the no metering scenario for CO_2, NO_x, CO, and HC emissions, respectively.

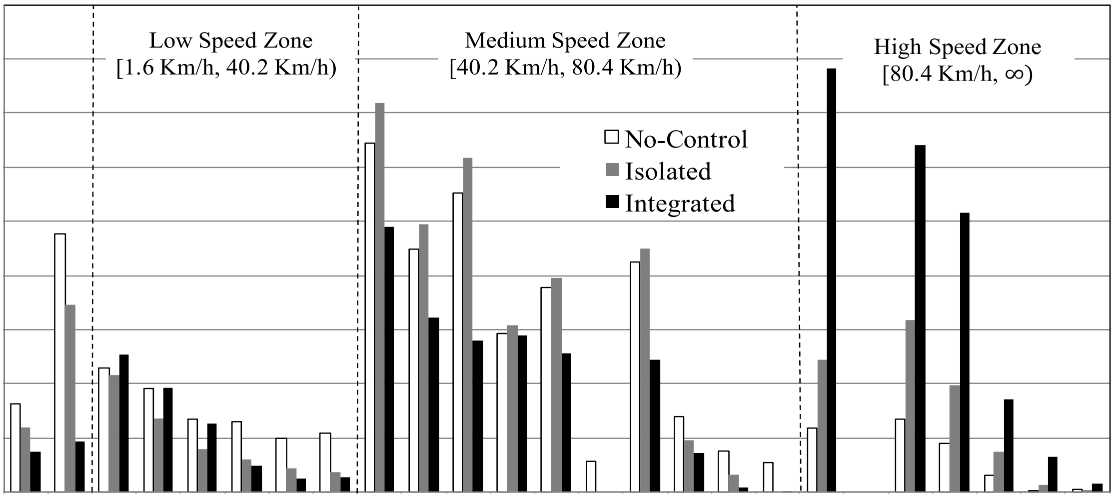

Fig. 5. Operational mode ID distributions

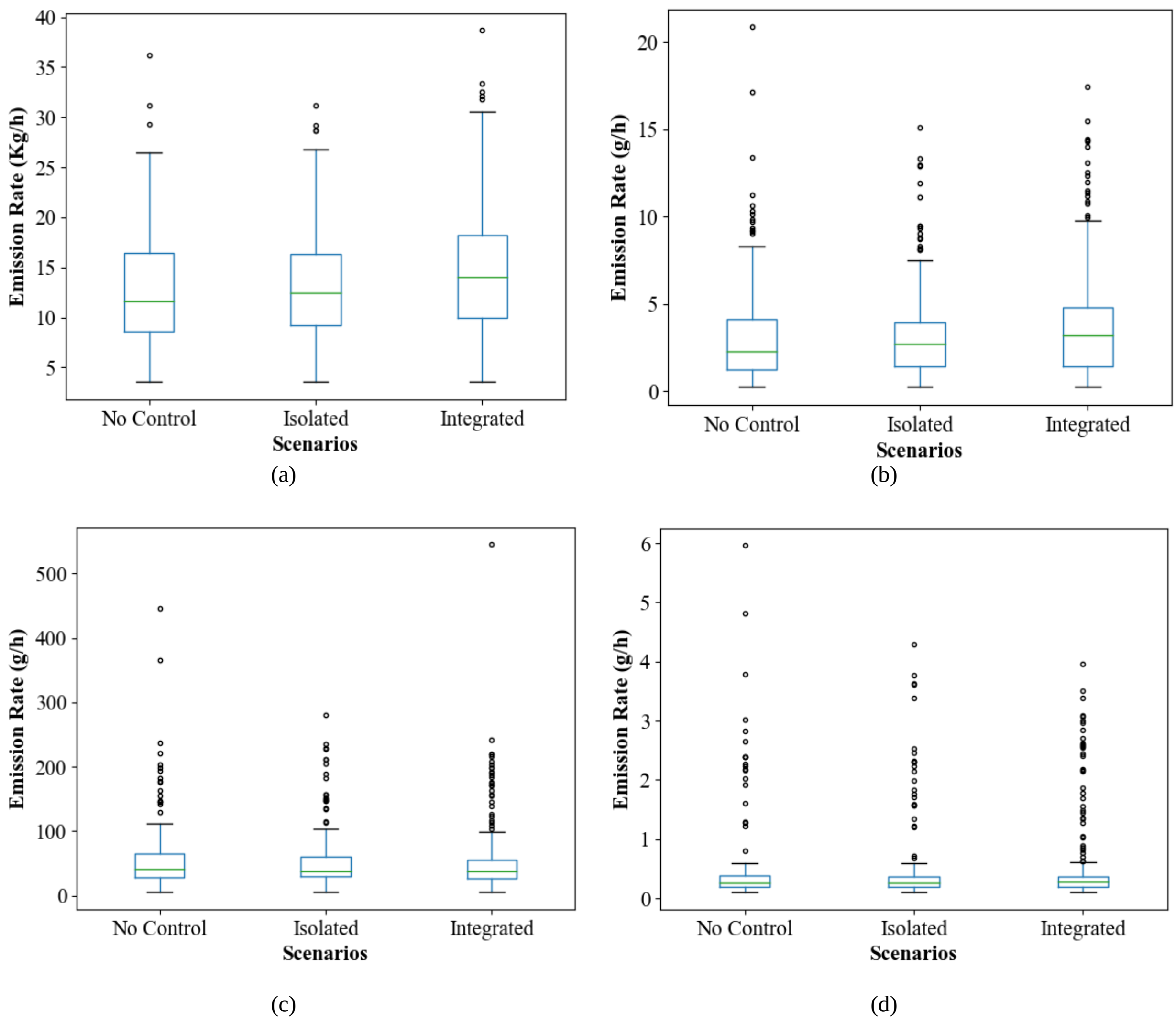

Fig. 6. Emission rate distributions in no metering, isolated, and integrated ramp metering scenarios: (a) CO_2 emission rates; (b) NO_x emission rates; (c) CO emission rates; (d) HC emission rates

Table 3. One-way ANOVA test results of emission rates and total emissions of three scenarios

One Way ANOVA Test on Emission Rates				
Pollutants	***CO_2***	***NO_x***	***CO***	***HC***
	p-value	***p-value***	***p-value***	***p-value***
No control vs. isolated metering	2.00E-18	1.31E-13	3.27E-05	3.06E-03
No control vs. integrated metering	2.49E-64	8.46E-37	1.12E-04	1.92E-06
Isolated vs. integrated metering	4.29E-16	8.06E-08	8.59E-01*	8.88E-02*
Total Emissions (g)				
Pollutants	***CO_2***	***NO_x***	***CO***	***HC***
No control	4,033.91	0.83	16.53	0.14
Isolated metering	4,276.84	1.04	18.2	0.16
Integrated metering	3,394.26	0.83	12.67	0.12

** insignificant difference at the conference level 97%*

However, the total emissions in the isolated scenario are overall higher than in the no metering scenario by 8.50%, 25.90%, 10.10%, and 14.29% for CO_2, NO_x, CO, and HC emissions, respectively. Though the isolated control could improve the mobility denoted by higher driving speeds, the consequent shorter trip duration is insufficient to offset the increasing emission rates due to the 10% higher distribution in the high speed zone. Recalling the operational mode distributions in Fig. 3, 17.5% and 7.5% of operational modes distribute to the high speed zone in the isolated and no metering scenarios, respectively.

5.7. Summary of ramp metering strategy performance

During rush hours of a weekday, the isolated and integrated ramp metering strategies could improve the mobility, therefore reducing travel delay; and prevent harder acceleration and deceleration from being operated. The integrated metering strategy is more beneficial to the mobility improvement and smooth vehicle maneuver than the isolated one, which is reflected by the dominant distribution of the operational mode IDs as well.

While only 17.5 % and 7.5 % of the operational mode IDs distribute to the medium speed zone in the no metering and isolated metering strategies, the dominant operational modes in the integrated control are observed in the high-speed zone with 43.8% distribution. As a result of the high distribution in the high-speed zone, the consequent emission rates are slightly higher in the integrated metering scenario. Despite of this, the total emissions in the integrated metering scenario are the lowest for the shorter emission duration. Nevertheless, compared to the no metering scenario, the mobility improvement by the isolated control is insufficient to compensate the higher emissions ascribed to the 10 % more distribution of operational mode IDs in the high-speed zone. Consequently, the total emission under the isolated ramp metering control is the highest.

6. Conclusions

Isolated and integrated ramp metering control strategies could improve mobility and enhance smooth vehicle maneuver in the mainline of a freeway. However, the ramp metering control strategy is not always favorable to vehicle emissions. The total emissions measured in the isolated ramp metering control strategy are higher than the no metering strategy in the test site. This might be because that, the improved mobility and the consequently shortened trip duration is insufficient to offset the increasing emission rates.

Only when the mobility is significantly improved, such as the one in the integrated ramp metering control strategy, the total emissions are tremendously reduced for the shorter emission duration. Therefore, the integrated ramp metering control strategy is superior to the isolated control strategy, in terms of both mobility and vehicle emissions. As the focus of this study is on the mainline freeway, the estimation of ramp emissions is not included at this moment.

Acknowledgments

The authors acknowledge that this research is supported in part by the National Science Foundation (NSF) under grants #1137732. The authors appreciate Michael Pietrzyk and Magdy Kozman in Texas Department of Transportation at Houston TranStar for the kind helps. The opinions, findings, and conclusions or recommendations expressed in this material are those of the author(s) and do not necessarily reflect the views of the funding agencies.

References

Arnold Jr. E.D., (1998), *Ramp metering: a review of the literature*, Virginia Department of Transportation, On line at: https://pdfs.semanticscholar.org/d991/df4730b7c1a4fcdfb22acf42d48f50d7fd8b.pdf.

Bhouri N., Haj-Salem H., Kauppila J., (2013), Isolated versus coordinated ramp metering: Field evaluation results of travel time reliability and traffic impact, *Transportation Research Part C: Emerging Technologies*, **28**, 155-167.

Brugge D., Durant J.L., Rioux C., (2007), Near-highway pollutants in motor vehicle exhaust: A review of epidemiologic evidence of cardiac and pulmonary health risks, *Environmental Health*, **6**, 23-23.

Carlson R.C., Papamichail I., Papageorgiou M., Messmer A., (2010), Optimal Motorway Traffic Flow Control Involving Variable Speed Limits and Ramp Metering, *Transportation Science*, **44**, 238-253.

Cassidy M.J., Rudjanakanoknad J., (2005), Increasing the capacity of an isolated merge by metering its on-ramp, *Transportation Research Part B: Methodological*, **39**, 896-913.

DHHS, (1994), NIOSH Pocket Guide to Chemical Hazards, U.S. Department of Health and Human Services, Centers for Disease Control and Prevention, National Institute for Occupational Safety and Health, On line at: https://search.library.wisc.edu/catalog/999770376202121.

EPA, (2011), Development of Emission Rates for Light-duty Vehicles in the Motor Vehicle Emissions Simulator (MOVES2010): Final Report, Assessment and Standards Division, Office of Transportation and Air Quality, U.S. Environmental Protection Agency, On line at: https://books.google.com/books?id=9MeFnQAACAAJ.

Franco V., Kousoulidou M., Muntean M., Ntziachristos L., Hausberger S., Dilara P., (2013), Road vehicle emission factors development: A review, *Atmospheric Environment*, **70**, 84-97.

Frey H.C., Liu B., (2013), *Development and Evaluation of Simplified Version of MOVES for Coupling with Traffic Simulation Model*, Proc. Transportation Research Board 92nd Annual Meeting, Washington, DC, .

Guang Y.X., Lei N., (2006), *Research on Evaluation of Expressway Ramp Isolated Metering Strategy in Shanghai*, Proc. of the 6th International Conference on ITS Telecommunications, 890-893.

Haines A., Kovats R.S., Campbell-Lendrum D., Corvalán C., (2006), Climate change and human health: impacts, vulnerability and public health, *Public Health*, **120**, 585-596.

Hall J., De Hurtado M.P., (1992), Effect of intersection congestion on accident rates, *Transportation Research Record*, **1**, 71-77.

Hansen J., Ruedy R., Sato M., Lo K., (2010), Global surface temperature change, *Reviews of Geophysics*, **48**, Rg4004.

Howard I.L., Warren K.A., (2009), Finite-element modeling of instrumented flexible pavements under stationary transient loading, *Journal of Transportation Engineering*, **135**, 53-61.

Jaafar M.N.M., (2016), Mitigation of gaseous emission from burner system utilizing envo diesel fuel via air staging method, *Environmental Engineering and Management Journal*, **15**, 873-878.

Kachroo P., Ozbay K., (2011), *Feedback Ramp Metering in Intelligent Transportation Systems*, Springer, Berlin Heidelberg New York, 169-340.

Li Q., Qiao F., Yu L., (2016), Vehicle emission implications of drivers smart advisory system for traffic operations in work zones, *Journal of the Air & Waste Management Association*, **66**, 446-455.

Li Q., Qiao F., Yu L., (2017a), Drivers' smart advisory system improves driving performance at STOP sign intersections, *Journal of Traffic and Transportation Engineering*, **4**, 262-271.

Li Q., Qiao F., Yu L., Chen S., Li T., (2017b), Impact of freeway weaving segment design on light-duty vehicle exhaust emissions, *Journal of the Air & Waste Management Association*, DOI: 10.1080/10962247.2017.1344744.

Li Q., Du J., Qiao F., Yu L., (2018), Characterizing Particulate Matter 2.5 concentration pattern within a transportation network: a case study in the port of Houston Region, *Journal of Pollution*, **1**, On line at: https://www.omicsonline.org/open-access/characterizing-particulate-matter-25-concentration-pattern-within-atransportation-network-a-case-study-in-the-port-of-houston-regi.pdf.

Liu S., Li Q., Qiao F., Du J., Yu L., (2017), Characterizing the relationship between carbon dioxide emissions and vehicle operating modes on roundabouts - a pilot test in a single lane entry roundabout, *Journal of Environment Pollution and Climate Change*, **1**, 1-8.

Luenberger D.G., (1973), *Introduction to Linear and Nonlinear Programming*, Springer, Berlin Heidelberg New York, 33-82.

Mahajan N., Hegyi A., Weg G.D., Hoogendoorn S.P., (2015), *Integrated Variable Speed Limit and Ramp Metering Control against Jam Waves - A COSCAL v2 Based Approach*, Proc. of the IEEE 18th Int. Conf. on Intelligent Transportation Systems, 1156-1162.

McCarthy J.E., Lattanzio R.K., (2015), *Ozone air quality standards: EPA's 2015 revision, congressional research service*, On line at: https://www.lankford.senate.gov/imo/media/doc/Ozone%20Air%20Quality%20Standards%20EPAs%202015%20Revision.pdf.

Nash S.G., Sofer A., (1996), *Linear and Nonlinear Programming*, McGraw-Hill, New York.

Papageorgiou M., Kotsialos A., (2000), *Freeway Ramp Metering: an overview*, Proc. of the IEEE Intelligent Transportation Systems Conf., 228-239.

Outapa P., (2017), Dynamic air toxic emission factor of motorcycles in bangkok, thailand, *Environmental Engineering and Management Journal*, **16**, 2823-2830.

Onofrei M., (2017), The impact of environmental tax reform on greenhouse gas emissions: empirical evidence from european countries, *Environmental Engineering and Management Journal*, **16**, 2843-2849.

Rosu L., Istrate M., Bănică A., (2018), Passenger car dependency and consequent air pollutants emissions in Iasi metropolitan area (Romania), *Environmental Engineering and Management Journal*, **17**, 865-875.

Papamichail I., Kampitaki K., Papageorgiou M., Messmer A., (2008), Integrated ramp metering and variable speed limit control of motorway traffic flow, *IFAC Proceedings Volumes*, **41**, 14084-14089.

Pasquale C., Sacone S., Siri S., (2014), *Ramp Metering Control for two Vehicle Classes to Reduce Traffic Emissions in Freeway Systems*, Proc. of the European Control Conf. (ECC), 2588-2593.

Pease K., (2010), Vehicle Range Finder. USA Patent, No. US20100138142A1.

Pierson W.R., Gertler A.W., Bradow R.L., (1990), Comparison of the SCAQS tunnel study with other on road vehicle emission data, *Journal of the Air & Waste Management Association*, **40**, 1495-1504.

Qiao F., (1991), Highway traffic operation system, *East China Highway*, **3**, 80-84.

Qiao F., Liu L., Long W., Yu L., (2014), *Impacts of Average Commuting Time on Housing Prices in Texas Suburban Cities*, Proc. of the Transportation Research Board 93th Annual Meeting No. 14-1754, On line at: https://trid.trb.org/view/1287959.

Qiao F., Hill L., Wang X., Yu L., (2015), Measurement of emissions from passenger-picking-up vehicles at airport terminals, *Journal of Environmental Science and Engineering*, **5**, 65-70.

Qiao F., Liu L., Long W., Li Q., Yu L., (2016), *Charactering the relationship between real estate values and commuting time: a case study in Texas suburban cities, urban planning and design research*, On line at: http://www.seipub.org/updr/paperInfo.aspx?ID=30722.

Shinar D., (2017), *Traffic Safety and Human Behavior*, Emerald Publishing Limited, Bingley, On line at: https://www.emeraldinsight.com/doi/abs/10.1108/978-

1-78635-221-720162027.
Su L., (2016), Emission characteristics of double swirl combustion system for a diesel engine, *Environmental Engineering and Management Journal*, **15**, 1611-1616.
Tang M., Gong D., Liu S., Lu X., (2017), Finding key factors affecting the locations of electric vehicle charging stations: a simulation and anova approach, *International Journal of Simulation Modelling*, **16**, 541-554.
Vitousek P.M., Mooney H.A., Lubchenco J., Melillo J.M., (1997), Human domination of Earth's ecosystems, *Science*, **277**, 494-499.
Weinhold B., (2011), Pollution portrait: the fourth national-scale air toxics assessment, *Environmental Health Perspectives*, **119**, 254-257.
Wu Y., Chen Y., Li W., Guo Y., (2017), *Ramp Metering of Freeway Network Based on Dynamic Graph Hybrid Automata*, Proc. of the 29th Chinese Control and Decision Conference (CCDC), 7045-7050.